Journal of Knot Theory and Its Ramifications

CLASSIFICATION OF GENUS 1 VIRTUAL KNOTS HAVING AT MOST 5 CLASSICAL CROSSINGS

A.A. AKIMOVA, S.V. MATVEEV

Department of Mathematics, Mechanics and Computer Science
South Ural State University, Chelyabinsk, Russia
akimova_susu@mail.ru

Chelyabinsk State University and Institute of Mathematics and Mechanics of
Ural branch of the Russian Academy of Sciences
matveev@csu.ru

ABSTRACT

The goal of this paper is to tabulate all genus one prime virtual knots having diagrams with ≤ 5 classical crossings. First we construct all nonlocal prime knots in the thickened torus $T \times I$ which have diagrams with ≤ 5 crossings and admit no destabilizations. Then we use a generalized version of the Kauffman polynomial to prove that all those knots are different. Finally, we convert the knot diagrams in T thus obtained into virtual knot diagrams in the plane.

Keywords: virtual knot, genus one, tabulation.

Mathematics Subject Classification 2000: 57M25, 57M27

1. Introduction

Virtual knot theory was developed by L. Kauffman in 1996, see [1]. This theory is close to the theory of knots in thickened surfaces, i.e., in manifolds of type $S \times I$, where S is a closed orientable surface and I is the interval $[0, 1]$. We tabulate all prime knots in the thickened torus $T \times I$ which have diagrams with ≤ 5 crossings and admit no destabilizations. According to G. Kuperberg's theorem [2], this is equivalent to the tabulation of prime genus one virtual knots having diagrams with ≤ 5 classical crossings. See [3 - 7] for tabulation of knots and tangle projections in different 3-manifolds, and [8] for a table of virtual knots. See also [9] for the prime decomposition theorem for virtual knots.

Let us describe the main ideas of the tabulation of prime knots in $T \times I$. We do this in three steps. First we compose a table of knot projections in T such that any prime knot in $T \times I$ having a minimal diagram with $m \leq 5$ crossings admits at least one projection which has m vertices and is contained in the table. To this end we use a kind of the second Reidemeister move called *biangle face addition*, see Fig. 4. It turns out that, with exactly 3 exceptions, any projection from the table having $m \leq 5$ vertices can be obtained by the above move from a not necessarily tabulated projection with $m-2 \leq 3$ vertices.

At the second step we convert each projections into the set of corresponding knot diagrams by supplying each vertex with an overpass-underpass indication. Of course, we reject all duplicates and non-prime knots.

Then we prove that the list of knots thus obtained contains no duplicates. We do that by calculating their generalized Kauffman polynomials. Fortunately, all of them turned out to be distinct.

At last, we convert the knot diagrams in T thus obtained into virtual knot diagrams in the plane.

2. Main Result

Recall that a virtual knot is an equivalence class of virtual knot diagrams modulo generalized Reidemeister moves. Virtual knots can also be defined as equivalence classes of knots in thickened surfaces up to homeomorphisms, stabilizations, and destabilizations. See [1, 10]. The genus of a virtual knot k is the minimal genus of a surface S such that K is situated in $S \times I$.

We consider genus one virtual knots, i.e., knots in $T \times I$ such that they admit no destabilizations. Knots in $T \times I$, as well as classical knots, can be represented by projections and diagrams. By a projection we mean a regular graph $G \subset T$ of degree 4 such that the "straight ahead" rule determines a cycle composed of all the edges of G. This cycle can be converted into a knot diagram by breaking it in each crossing point to show which strand is going over the other with respect to the coordinate function on I. Two projections G, G' are called equivalent if the pairs (T, G), (T', G') are homeomorphic. The diagram equivalence has the same meaning. We also allow simultaneous crossing changes at all crossings, which corresponds to homeomorphism $h\colon T \times I \to T \times I$ induced by the nontrivial symmetry $\varphi\colon I \to I$.

Definition 2.1. A diagram of a knot $K \subset T \times I$ is called minimal if its complexity (the number of crossings) is not more than the complexity of every diagram of every knot equivalent to K. A projection $G \subset T$ is minimal if at least one of the corresponding knot diagrams is minimal.

Definition 2.2. We say that a knot $K \subset T \times I$ is composite if at least one of the following holds:

- K is a connected sum of a nontrivial (i.e., not bounding a disc) knot in $T \times I$ and a nontrivial knot in S^3.
- K is a nontrivial circular connected sum of two knots in $T \times I$, see [10, 11]. This means that there exist two disjoint essential annuli in $T \times I$, which decompose $T \times I$ into two copies of the standard thickened annulus $A \times [0, 1]$ such that K intersects each copy along a nontrivial arc joining $A \times \{0\}$ with $A \times \{1\}$. Here we

call an arc $l \subset A \times [0,1]$ trivial if there is an isotopy $A \times [0,1] \to A \times [0,1]$ which is invariant on $A \times \{0,1\}$ and takes l to an arc of the type $\{*\} \times [0,1]$.

Definition 2.3. We say that a knot projection $G \subset T$ is composite if at least one of the following holds:

- There is a disc $D \subset T$ such that $\partial D \cap G$ crosses the edges of G transversely at two points and the intersection $G \cap D$ contain a vertices of G.
- For any two disjoint nontrivial circles in T such that each crosses the edges of G transversely at one point both annuli into which the circles decompose T contains a vertex of G.

It is easy to see that all diagrams corresponding to composite projections can determine only composite knots.

Definition 2.4.
We say that a knot $K \subset T \times I$ is prime if it is noncomposite and admits no destabilization. A projection (or a diagram) is prime if it corresponds to some prime knot in $T \times I$.

It is convenient to think of T as a square with identified opposite sides. So we will represent projections and diagrams of knots in $T \times I$ by collections of proper arcs in squares such that the identifications of opposite sides respect the endpoints of the arcs.

Theorem 2.5. *There exist exactly 90 different prime knots in $T \times I$ having diagrams with at most 5 crossings. The diagrams of these knots are shown in Fig. 15 at the end of the paper.*

We say that a virtual knot is composite if it can be represented as the connected sum of two nontrivial virtual knots. See [10] for the definition of the connected sum of virtual knots. Nontrivial virtual knots that are not composite are called prime.

It follows from the Kuperberg theorem [2] that there is a natural bijection between genus one virtual knots and knots in $T \times I$ admitting no destabilization. This bijection respects connected summations. Therefore, the following theorem, which we consider as the main result of this paper, is equivalent to Theorem 2.5.

Theorem 2.6. *There exist exactly 90 different prime genus one virtual knots having diagrams with at most 5 classical crossings. Diagrams of these knots are shown in Fig.16 at the end of the paper.*

3. Enumeration of Projections in T

Lemma 3.1. *There exist exactly 11 abstract regular graphs of degree 4 having at most* 5 *vertices and no loops, see Fig. 1.*

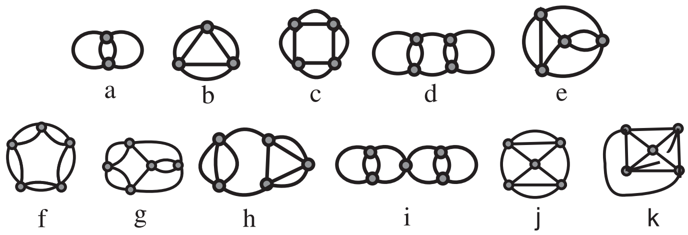

Fig. 1. Regular graphs of degree 4 having at most 5 vertices and no loops.

Proof. Let G_n be a degree 4 regular graph having $n \leq 5$ vertices. We claim that if G_n differs from the graph k (which is a complete graph with 5 vertices), then G_n has either a loop or a multiple edge. Indeed, if G_n has no loops and multiple edges then G_n embeds into the complete graph K_n with n vertices. Since G_n and K_n have $2n$ and $n(n-1)/2$ edges respectively, we get the inequality $2n \leq n(n-1)/2$. For $n \leq 5$ this inequality holds only for $n = 5$, when $G_n = k$. It follows that all other degree 4 regular graphs with $n \leq 5$ vertices and no loops can be obtained from a circle by a few (in fact, ≤ 4) operations of the following two types: 1) addition of a loop, and 2) addition of a multiple edge. Performing these operations and removing duplicates, we get graphs $a - j$ in Fig. 1. □

Theorem 3.2. *There exist exactly 47 different prime projections in T with at most 5 crossings, see Fig. 2.*

We decompose the proof into several steps.

STEP 1. Let G be a projection of type a, see Fig. 1. Then G can be represented as the union of two circles having two intersection points such that exactly one of them is transverse. Let l_1, l_2 be small arcs of the circles containing the non-transverse intersection point. Remove this point by the operation shown in Fig. 3. The dashed line α shows how to perform the inverse operation. We get a pair of circles which have only one transverse intersection point and thus can be considered as a meridian-longitude pair for T. Since the complement to the circles is a disc, there is only one way of restoring G. Applying this operation to the standard meridian-longitude pair for T, we get a unique prime projection $\mathbf{2_1}$ of type a.

STEP 2. Let us prove that there are no prime projections of types d, h, i. Indeed, any projection $G \subset T$ of types d, h, or i has a triple edge E, i.e., two vertices v_1, v_2 joined by three edges. Let us join v_1, v_2 by a simple path $l \subset G$ composed of two or three edges of G. We get a regular graph $G' = E \cup l \subset G$ of type a. Note that the union of the first and last edges of l separates G. It follows that G' is a projection, which is equivalent to 2_1 and thus has the complement consisting of two discs. It remains to verify that there are no way to insert the remaining edges of G into

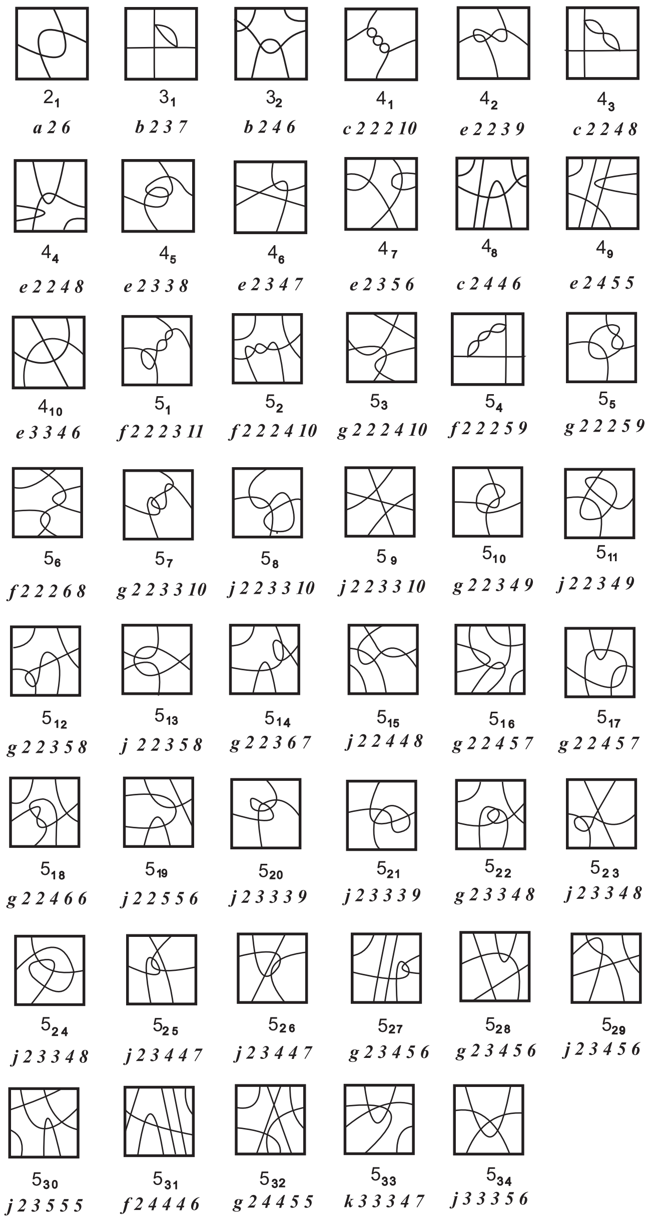

Fig. 2. Prime projections with at most 5 crossings in T represented as squares with identified opposite sides. Each string of the type $\{x\ i_1\ i_2\ \dots\ i_n\}$ means that the corresponding projection is of type $x \in \{a, b, c, d, e, f, g, h, k\}$ and that its faces are i_m-polygons for $1 \leq m \leq n$.

those discs so as to get a prime projection.

STEP 3. Let G be a projection of type b, see Fig. 1. It consists of 3 circles such

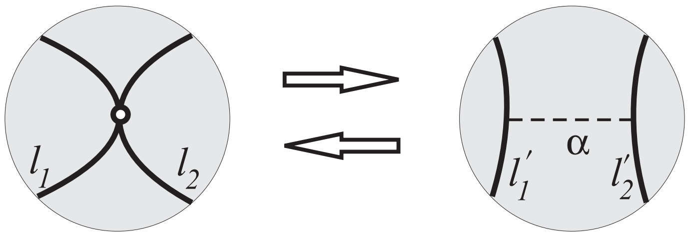

Fig. 3. Removal of a nontransverse point. If we contract the dashed line to a point, we restore the original projection.

that any two of them have a common point. Suppose that the intersection point of two circles is transverse. Then they form a meridian-longitude pair of T. Since the complement to the circles is a disc, there is only one way of restoring G by adding the third circle. Applying such addition to the standard meridian-longitude pair for T, we get a unique prime projection $\mathbf{3_1}$ of type b.

STEP 3.1. Now we suppose that all intersection points of the circles are not transverse. Just as in STEP 1 we replace all of them by dashed arcs as shown in Fig. 3. We get a cyclically ordered collection of three disjoint circles in T such that each circle is joined with the next one by a dashed line. The lines are also disjoint. If we contract them to points, we recover G. Denote by t the number of trivial circles among the above three. It is easy to see that if $t = 1$ then G is equivalent to the projection $\mathbf{3_2}$. In all other cases we get either a non-prime projection (if $t = 3$) or projections of links (if $t = 0$ or $t = 2$).

STEP 4. In order to classify prime knot projections in T with 4 and 5 vertices, we shall use the following method. Suppose that a knot projection G with n vertices has two disjoint biangle faces. Let us remove each of them by performing a kind of the second Reidemeister move, which is shown in Fig. 4 and is denoted L. We get a projection G', which has $n - 4$ vertices and is equippped with two disjont dotted arcs α_1, α_2 connecting the corresponding edges of G'. Of course, G can be obtained from G' by performing the inverse moves L^{-1} along l_1 and along l_2. If G is prime, we call the arcs α_1, α_2 *appropriate*.

In order to obtain all prime projections with n vertices admitting two disjoint biangle faces, it suffices to do the following:

(1) Enumerate all projections with $n - 4$ vertices;
(2) For each projection find out all appropriate pairs of dotted arcs.
(3) For each pair of appropriate dotted arcs construct the corresponding projection by performing L^{-1} along these arcs.

Since the arcs are appropriate, they must possess the following properties:

- The union of G' and the dotted arcs decomposes T into discs. Otherwise G would be reducible.

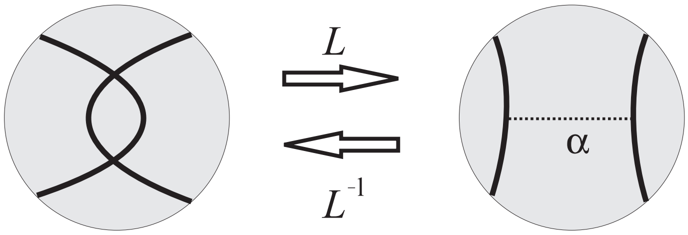

Fig. 4. L removes biangle faces while L^{-1} along the dotted arc α produces them.

- If G' has a loop, then this loop must contain an endpoint of the dotted arc. Otherwise the loop would survive by restoring G.

The same method works for constructing projections which possess only one biangle face or two biangle faces having a common vertex. The difference is that in this case we use only one move L, which decreases the number of vertices by 2. Also, if G' has a biangle face, then the boundary of this face must contain an endpoint of the dotted arc. Otherwise G would have two biangle faces: the biangle face of G' and the biangle face appearing by performing G.

STEP 4.1. Let G be a projection of types c or e. Suppose G has two disjoint biangle faces. Let us remove them by two moves L. We get a projection G', which has no vertices and thus is a circle in T. We get also a pair of disjoin dotted arcs responsible for recovering G. If G' is trivial in T, then up to equivalence relation generated by homeomorphisms $(T, G') \to (T, G')$, there is only one pair of dotted arcs producing a prime projection, which is $\mathbf{4_4}$. In the case when G' is nontrivial, there are two nonequivalent appropriate pairs of dotted arcs producing projections $\mathbf{4_1}$ and $\mathbf{4_2}$. See the first 3 squares in Fig. 5 for the dotted arcs and Fig. 2 for the corresponding projections.

STEP 4.2. Suppose that G has a biangle face but does not have two disjoint biangle faces. Removing that biangle face, we get a projection G' with 2 vertices and one dotted arc. There are two regular graphs with 2 vertices: the graph b and the nonclosed chain of 3 circles, which we denote c_3.

Let us consider the first case. According to STEP 1, there is only one projection of type b. Let us call a dotted arc joining two points inside edges of G' appropriate if it produces a prime projection without disjoint biangle faces. Note that any dotted arc must lie in a face of G'. Moreover, at least one end of some appropriate dotted arc must lie in a boundary edge of the biangle face of G' (otherwise G would have two disjoint biangle faces). Considering all possible positions of appropriate dotted arcs inside the faces (see the last 3 squares in Fig. 5), we get the projections $\mathbf{4_3}$, $\mathbf{4_6}$,$\mathbf{4_8}$ shown in Fig. 2.

STEP 4.3. Now suppose that G' is a nonclosed chain of 3 circles. Both intersection points of the circles are nontransverse, because otherwise G' would be a projection of a link. Let us remove these points as shown in Fig. 3. We get 3 disjoint circles joined by two dashed lines. The circles cannot be nested. Up to homeomorhisms $T \to T$, there are exactly 7 mutual positions of circles und dashed lines. See Fig. 6 for the corresponding projections. The first 4 admit no appropriate dotted arc. Each of the remaining 3 projections has exactly one appropriate dotted arc. In this way we get projections $\mathbf{4_2}$, $\mathbf{4_7}$, $\mathbf{4_9}$, see Fig. 2.

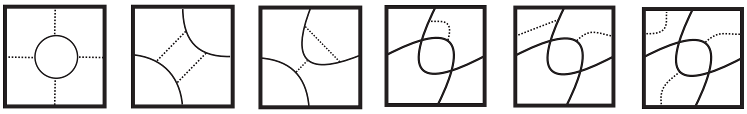

Fig. 5. Dotted arcs producing 9 prime projections with 4 vertices

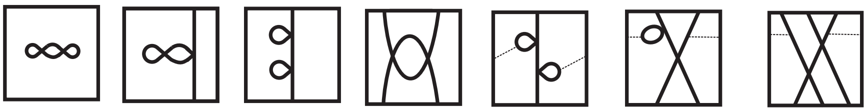

Fig. 6. Projections of the type c_3

STEP 4.4. Suppose that G has no biangle faces. Then its double edges form two disjoint nontrivial circles in T, which decompose T into two annuli. The remaining four edges are contained in these annuli (m edges in the first annulus, n in the second one). We cannot have $(m, n) = (0, 4)$ or $(2, 2)$, because otherwise G would either admit a destabilization or be a projection of a link. In the case $(m, n) = (1, 3)$ we get the projection $\mathbf{4_{10}}$.

STEP 5. Consider a projection G of types f, g, or j.

STEP 5.1. Suppose that G has 2 disjoint biangle faces. Removing them we get a projection G' having one vertex and two loops. If both loops are trivial, there are two appropriate pairs of dotted arcs. They produce the projections $\mathbf{5_{14}}$ and $\mathbf{5_{19}}$. If only one loop is trivial, there are 9 appropriate pairs of dotted arcs. They determine the projections $\mathbf{5_1}$, $\mathbf{5_4}$, $\mathbf{5_5}$, $\mathbf{5_7}$, $\mathbf{5_8}$, $\mathbf{5_{11}}$, $\mathbf{5_{13}}$, $\mathbf{5_{16}}$ and $\mathbf{5_{17}}$. At last, if both loops are nontrivial, we get the projections $\mathbf{5_2}$, $\mathbf{5_3}$, $\mathbf{5_6}$, $\mathbf{5_9}$, $\mathbf{5_{12}}$, $\mathbf{5_{15}}$. See Fig. 7 for appropriate dotted arcs and Fig. 2 for the corresponding projections.

STEP 5.2. Suppose that G has a biangle face but does not have two disjoint biangle faces. Removing one biangle face we get a projection G', which has 3 vertices

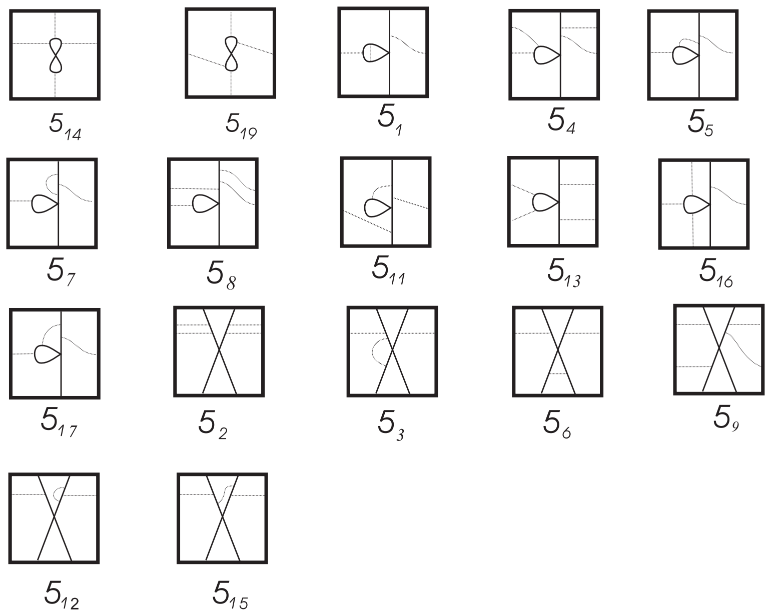

Fig. 7. Projections with one vertex admitting appropriate pairs of dotted arcs

and ≤ 2 loops, and thus is of type a_1, a_2, or b, see Fig. 8.

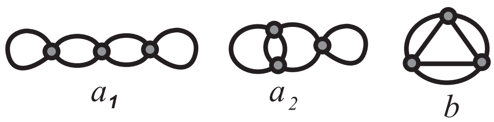

Fig. 8. Regular graphs with 3 vertices and ≤ 2 loops.

Suppose that G' is of type a_1, i.e., a chain of 4 circles. Each circle is either trivial in T or not. Denote by t the number of trivial circles. We cannot have $t > 2$, since each circle must contain an endpoint of the dotted arc. For each value of t from 2 to 0 there is only one projection of type a_1 admitting an appropriate dotted arc, and this arc is unique. Performing the move L^{-1}, we get the projections $\mathbf{5_{22}}$, $\mathbf{5_{27}}$, $\mathbf{5_{32}}$.

Suppose G' is of type a_2. Then G' can be obtained from the projection 2_1 (see Fig. 1) by adding a trivial loop. There are 3 cases.

(1) The loop is placed in the biangle face of G'. Denote this face F. Then there is only one appropriate dotted line, which produces the projection $\mathbf{5_{20}}$.

(2) The loop lies outside F but its vertex is in ∂F. Then there are 3 appropriate dotted arcs. They determine the projections $\mathbf{5_{21}}$, $\mathbf{5_{23}}$, $\mathbf{5_{30}}$.

(3) The loop lies outside F and its vertex is not in ∂F. In this way we get 2 appropriate dotted arcs and 2 corresponding projections $\mathbf{5_{24}}$, $\mathbf{5_{25}}$. See Fig. 9 for the appropriate dotted arcs and Fig. 4 for the corresponding projections.

Let G' be of type b. It consists of 3 circles such that any two of them have a common point. Suppose that the intersection point of two circles is transverse. Then just as in STEP 3 one can show that G' is equivalent to the projection $\mathbf{3_1}$. There are 4 inequivalent ways to draw a dotted arc, but only 3 of them determine inequivalent projections, which are $\mathbf{5_{10}}$, $\mathbf{5_{26}}$, $\mathbf{5_{28}}$. Now we suppose that all intersection points of the circles are not transverse. Just as in STEP 1 we replace all of them by dashed lines as shown in Fig. 3. We get a cyclically ordered collection of three disjoint circles in T such that each circle is joined with the next one by a dashed line. The lines are also disjoint. If we contract them to points, we recover G. Denote by t the number of trivial circles among the above three. It is easy to see that if $t = 1$ then G is equivalent to the projection 3_2 in Fig. 2. There are 4 appropriate dotted arcs. They determine 3 new projections $\mathbf{5_{31}}$, $\mathbf{5_{18}}$, $\mathbf{5_{29}}$, and the projection $\mathbf{5_2}$, which appeared earlier. In all other cases we get either a nonprime projection (if $t = 3$) or projections of links (if $t = 0$ and $t = 2$). See Fig. 9.

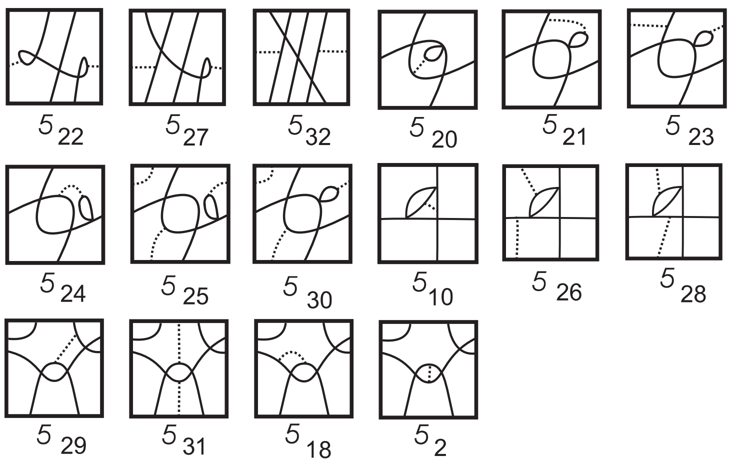

Fig. 9. Projections with 5 vertices which have a biangle face but do not have two disjoint biangle faces.

STEP 5.3. Suppose that G has no biangle faces. Since each of the graphs f, g, j has two disjoint double edges, G contains two disjoint nontrivial circles, which decompose T into two annuli A_1 and A_2. Each circle contains two vertices of G, the remaining vertex lies in the interior of one of the annuli, say, in A_1. Denote m and n the numbers of edges inside A_1 and A_2. Then $m \geq 4$ and $m + n = 6$. We cannot have $(m, n) = (6, 0)$ or $(4, 2)$, because otherwise G would either admit a destabilization or be a projection of a link. In the case $(m, n) = (5, 1)$ we get the prime projection $\mathbf{5_{34}}$, see Fig. 2.

STEP 6. Now we consider a prime projection G of type k, see Fig. 1. Note that G has 5 faces and that the total number of angles of faces of G is 20. Taking into account that G has no biangle faces, one can easily show that G has either a quadrilateral face Q or at least three triangle faces.

STEP 6.1. Suppose that G has a quadrilateral face Q. Then Q and two edges x, y joining the opposite vertices of Q form a kind of a meridian-longitude pair of T, see Fig. 10 to the left. Thus the complement to $x \cup y \cup Q$ in T is a disk containing the

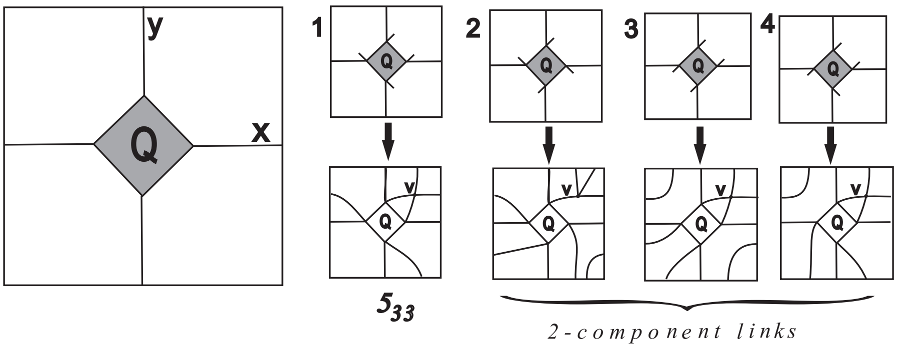

Fig. 10. The unique prime projection $\mathbf{5_{33}}$ of type k

remaining vertex v of G and 4 edges joining v with the vertices of Q. For each vertex w of Q there are exactly two nonisotopic arcs joining w with v. It is convenient to specify one of them by showing its small initial segment. Altogether there are 16 different choices of the segments. Nevertheless, since the pair $(T, x \cup y \cup Q)$ is very symmetric, one can reduce the number of choices to only 4 cases, see Fig. 10 to the right. Three of them determine projections of links, and only one determines the knot projection $\mathbf{5_{33}}$ of type k.

STEP 6.2. Now suppose that G has 3 triangle faces. It is easy to verify that for any three triangle cycles in the complete graph k on 5 vertices at least two of them have a common edge. It follows that there are two triangle faces of G having a common edge. Their union Q_1 is a quadrilateral in T. Denote its vertices by A, B, C, D such that (AC) is the common edge of those faces. Let v be the remaining vertex of G. Then the union μ of the edges (vA, AC, Cv) of G and the union λ of the edges $(AB), (BD), (DA)$ of G form a meridian-longitude pair of T. The remaining two edges (vB) and (vD) must approach to μ from the same side and to λ from the different sides, because otherwise G would be a projection of a link. The only way to get a projection of a knot is shown in Fig. 11. This projection has a quadrilateral face (shaded). According to Step 6.1, it is equivalent to the projection $\mathbf{5_{33}}$.

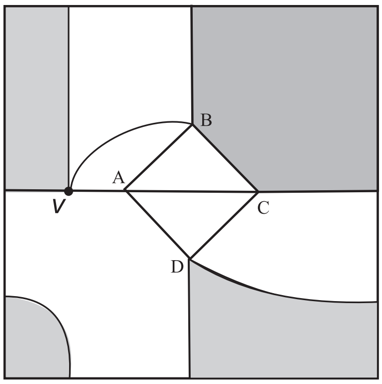

Fig. 11. This projection is equivalent to the one shown in Fig. 10

STEP 7. Let us prove that all projections in Fig. 2 are nonequivalent. With exactly 6 exceptions any two of them can be distinguished by their types and collections of faces indicated below each projection. There are 6 exceptional pairs of projections having identical types and faces. They are $(\mathbf{5_8}, \mathbf{5_9})$, $(\mathbf{5_{16}}, \mathbf{5_{17}})$, $(\mathbf{5_{20}}, \mathbf{5_{21}})$, $(\mathbf{5_{23}}, \mathbf{5_{24}})$, $(\mathbf{5_{25}}, \mathbf{5_{26}})$, and $(\mathbf{5_{27}}, \mathbf{5_{28}})$.

Let us prove that these projections are indeed different. We shall say that an edge e of a projection G has type $(3, 3)$ or $(3, 4)$ if it is a common edge either of two triangle faces of G or of a triangle and a quadrilateral faces of G respectively.

- The projections $\mathbf{5_8}, \mathbf{5_9}$ are different since one of them contains a type $(3, 3)$ edge while the other does not. The same is true for the projections $\mathbf{5_{25}}$ and $\mathbf{5_{26}}$.
- The projections $\mathbf{5_{16}}, \mathbf{5_{17}}$ are different since one of them contains an edge of type $(2, 4)$ while the other does not. The same is true for the projections $(\mathbf{5_{23}}, \mathbf{5_{24}})$, and $(\mathbf{5_{29}}, \mathbf{5_{28}})$.
- The projection $(\mathbf{5_{20}}, \mathbf{5_{21}})$ are different since each of the three triangle faces of $\mathbf{5_{20}}$ has a common point with its biangle face while $\mathbf{5_{21}}$ has a triangle face having no common points with the biangle.

4. How to prove Theorems 2.5 and 2.6?

We prove these theorems as follows. First we list all minimal diagrams of knots in T having projections shown in Fig. 2. Then we contsruct plane diagrams of the corresponding virtual knots. At last we prove that all knots thus obtained are different.

4.1. *Enumeration of Diagrams in T*

Let P be one of the projections listed in Fig. 2. We can recover all corresponding diagrams by indicating the types of the crossings of P in all 2^n possible ways, where n is the number of vertices of P. However one can essentially reduce this procedure by using the following ideas.

- The simultaneous crossing changes at all crossings convert any diagram to an equivalent one. Therefore, for any projection with n vertices it suffices to consider only 2^{n-1} possibilities.
- Let a fragment F of P be of types A_1, A_2, A_3, or A_4, see Fig. 12. One may think of it as the union of transverse arcs. After indicating crossing point the arcs become the arcs of the corresponding knot diagram. It is easy to see that each of them must be alternating, i.e. overcrossings must alternate with undercrossings as we go along the arc. Indeed, nonalternating diagrams of types $A_1 - A_4$ admit simplifications as shown for the fragment A_3. It follows that each A_i can be converted into a fragment of the corresponding knot diagram only in two ways. Implementation of the above made it possible to reduce the construction of the diagrams to reasonable size. The resulting table is shown in Fig. 15.

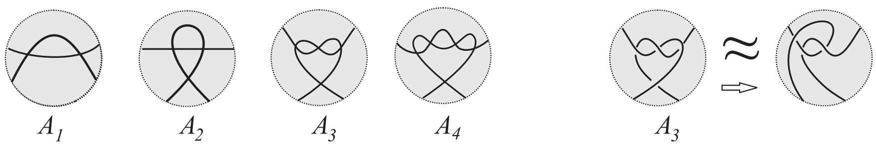

Fig. 12. Fragments of types $A_1 - A_4$ must be alternating

4.2. *Construction of plane Diagrams of virtual knots*

There are two equivalent definitions of virtual knots [1,10]: by knots in thickened surfaces and by plane diagrams with classical and virtual crossings. Recall that two virtual knot diagrams determine the same virtual knot if they are related by a sequence of generalized Reidemeister moves. These moves are classical Reidemeister moves $\Omega_1, \Omega_2, \Omega_3$, their virtual versions $\Omega_1', \Omega_2', \Omega_3'$, and the semi-virtual version Ω_3'' of Ω_3. In Fig. 13 we also show two useful combinations of those moves.

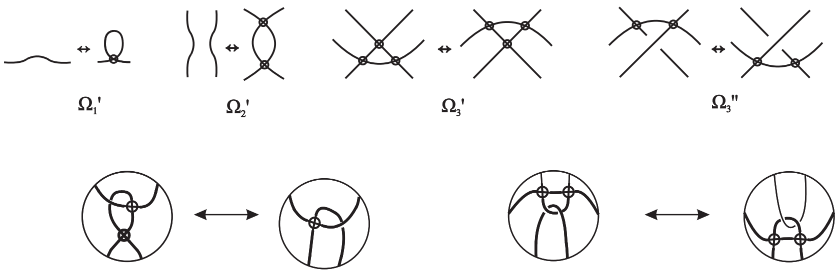

Fig. 13. Virtual versions of Reidemeister moves $\Omega_1', \Omega_2', \Omega_3'$, semi-virtual version Ω_3'' of Ω_3 and their useful combinations

In order to convert a square diagram of a knot in T into a plane diagrame of the corresponding virtual knot we perform the following two steps. First we close diagrams in in squares by analogy with the braid closure. The intersection of the new arcs consists of virtual crossings. Then we apply moves shown in Fig. 13 in order to remove suprfluous virtual crossings. See Fig. 14 for an example of converting the diagram 3_2 in T to a virtual plane diagram of the same knot.

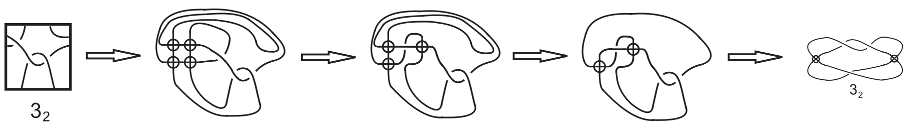

Fig. 14. An example

Applying this procedure to all knots in Fig. 15, we get the table of the corresponding virtual diagrams, see Fig. 16.

4.3. *How to prove that the above knots are different?*

In order to prove the knots are different we use the generalized Kauffman polynomial, which is slightly different from the usual normalized Kauffman bracket [12]. The exact formula is the following:

$$X(K) = (-a)^{-3w(K)} \sum_s a^{\alpha(s)-\beta(s)}(-a^2 - a^{-2})^{\gamma(s)} x^{\delta(s)}, \tag{4.1}$$

where $\alpha(s)$ and $\beta(s)$ are the numbers of markers A and B in a given state s, and $\gamma(s)$, $\delta(s)$ are the numbers of trivial and nontrivial circles in T obtained by resolving all crossing points. Just as for the original Kauffman polynomial, the sum is taken over all states. Of course, $w(K)$ is the writhe of the diagram. Direct manual and computer calculations showed that all Kauffman polynomials are of the above knots are different, See Table 1. Therefore the corresponding knots are also are different.

Acknowledgments

The first author is partially supported by the RFBR grant 12-01-00748 and the leading scientific schools grant 1015.2014.1.

The second author is partially supported by Laboratory of Quantum Topology of Chelyabinsk State University (Russian Federation government grant 14.Z50.31.0020) and the grant 12-T-1-1003/2 of Math. Branch of RAS.

References

[1] L.H. Kauffman, Virtual knot theory, *Eur. J. Comb.* **V. 20, N.7** (1999) 663–691.
[2] Greg Kuperberg, What is a virtual link? *Algebraic and Geometric Topology*, **V.3** (2003) 587 – 591.
[3] Yu.V. Drobotukhina, Jones polynomial analog for links in RP^3 and the generalization of Kauffman – Murasugi theorem, *Algebra and analysis* **V.2, N.3** (1991) 613 – 630.
[4] Yu.V. Drobotukhina, Classification of links in $\mathbb{R}P^3$ with at most six crossings, *Advances in Soviet Mathematics* **V.18, N.1** (1994) 87 – 121.
[5] B. Gabrovsek, M. Mroczkowski, Knots in the solid torus up to 6 crossings, *Journal of Knot Theory and Its Ramifications* **V.21, N.11** (2012) 43 pp.
[6] A.A. Akimova, S.V. Matveev, Classification of knots in $T \times I$ with at most 4 crossings, *Vestnik NSU* **V.12, N.3** (2012).
[7] A. Bogdanov, V. Meshkov, A. Omelchenko, M. Petrov, Enumerating the k-tangle projections, *J. of Knot Theory and its Ramifications*, **V.21, N.7** (2012) 17 pp.
[8] J. Green, A table of virtual knots, <*www.math.toronto.edu/drorbn/Students/GreenJ*>.
[9] S. Matveev, Ph. Korablev, Reductions of Knots in Thickened Surfaces and Virtual Knots, *Doklady Mathematics* **V.83, N.2** (2011) 262-264.
[10] V.O. Manturov, Knot theory, *CRC Press* (2004), 416 pp.
[11] S.V. Matveev, S.V. Prime decompositions of knots in $T \times I$, *Topology and its Applications* **V.159, N.7**(2011) 18201824.
[12] L.H. Kauffman, State models and the Jones polynomial, *Topology* **V.26, N.3** (1987) 395 – 407.

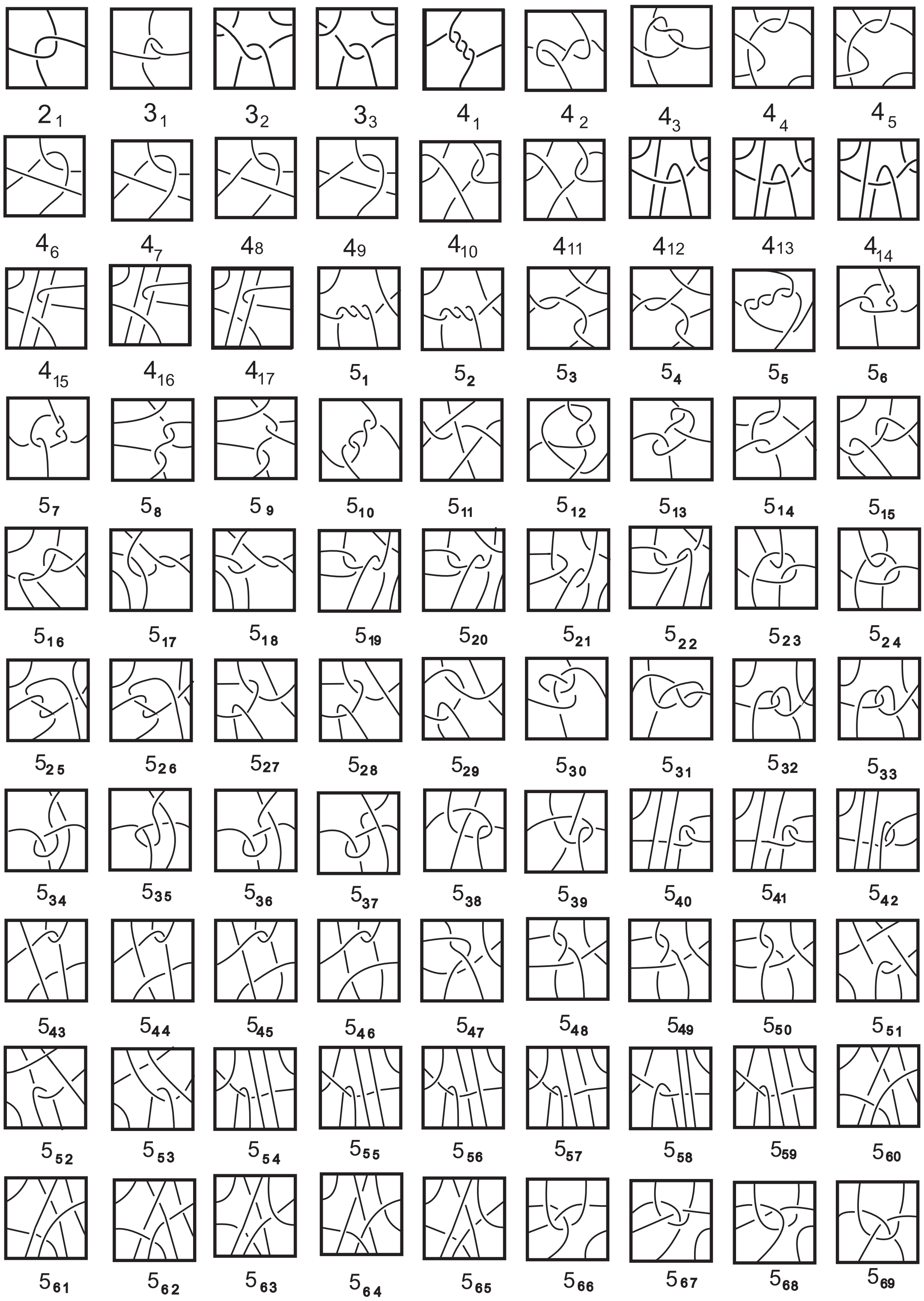

Fig. 15. Diagrams of nonlocal prime knots in $T \times I$ having diagrams with at most 5 classical crossings, where T is represented as a square with identified opposite sides

Table 1. Kauffman polynomials of knots shown in Fig. 15

$\mathbf{2_1}: (a^{-4}+a^{-6}-a^{-10})x$
$\mathbf{3_1}: (1+a^{2}-a^{-2}-a^{-4}+a^{-8})x$
$\mathbf{3_2}: 2a^{-6}+a^{-10}-a^{-14}+(-a^{-6}-a^{-10}+a^{-14})x^2$
$\mathbf{3_3}: a^{2}+2a^{-2}-a^{-10}+(-2a^{-2}+a^{-6})x^2$
$\mathbf{4_1}: (a^{-8}+a^{-10}-a^{-14}+a^{-18}-a^{-22})x$
$\mathbf{4_2}: (a^{-4}-a^{-8}+2a^{-12}+a^{-14}-a^{-16}-a^{-18})x$
$\mathbf{4_3}: (a^{-4}+a^{-6}-a^{-8}-a^{-10}+a^{-12}+a^{-14}-a^{-18})x$
$\mathbf{4_4}: -a^{-2}+a^{-6}+a^{-10}-2a^{-14}-a^{-18}+(-2a^{-10}+2a^{-14})x^2$
$\mathbf{4_5}: a^{6}-2a^{2}-2a^{-2}+a^{-6}+(-a^{6}+a^{2}+a^{-2}-a^{-6})x^2$
$\mathbf{4_6}: (a^{-14}-2a^{-10}-a^{-8}+a^{-6}+2a^{-4})x$
$\mathbf{4_7}: (a^{-16}-a^{-14}+a^{-12}+a^{-10}+a^{-8})x$
$\mathbf{4_8}: (2-a^{-4}+a^{2}-a^{6})x$
$\mathbf{4_9}: (-a^{-12}-a^{-10}+a^{-8}+2a^{-6}+a^{-4}-a^{-2})x$
$\mathbf{4_{10}}: 2a^{6}-a^{-2}+a^{-6}+(-a^{6}+a^{-2}-a^{-6})x^2$
$\mathbf{4_{11}}: a^{2}+a^{-2}-a^{-6}+a^{-14}+(-2a^{-2}+2a^{-6}-a^{-10})x^2$
$\mathbf{4_{12}}: (a^{-8}-2a^{-14}+2a^{-18})x+(a^{-14}-a^{-18})x^3$
$\mathbf{4_{13}}: (-a^{-2}+a^{-4}+a^{-14})x+(a^{-6}-a^{-10})x^3$
$\mathbf{4_{14}}: (1-a^{6}-a^{2}+a^{-2}+a^{-6})x+(a^{2}-a^{-2})x^3$
$\mathbf{4_{15}}: (-1-a^{-4}+a^{-6}-a^{-8}-a^{-10})x+a^{-4}x^3$
$\mathbf{4_{16}}: (-1-a^{4}+a^{2}-a^{-2}-2a^{-4}+a^{-8})x+x^3$
$\mathbf{4_{17}}: (-3a^{-8}+a^{-12}+a^{-14}-a^{-16}-a^{-18})x+a^{-8}x^3$
$\mathbf{5_1}: -a^{-26}+a^{-14}+2a^{-10}+(a^{-26}-a^{-22}+a^{-18}-a^{-14}-a^{-10})x^2$
$\mathbf{5_2}: -a^{-22}+2a^{-6}+a^{-2}+(a^{-18}-a^{-14}+a^{-10}-2a^{-6})x^2$
$\mathbf{5_3}: -a^{-22}+2a^{-18}+a^{-14}-a^{-10}+a^{-6}+(a^{-22}-a^{-18}-a^{-14}+a^{-10}-a^{-6})x^2$
$\mathbf{5_4}: a^{-10}+2a^{-6}-a^{-2}+a^{6}-a^{10}+(-2a^{-6}+2a^{-2}-a^{2})x^2$
$\mathbf{5_5}: (1+a^{-16}-a^{-12}-a^{-10}+a^{-8}+a^{-6}-a^{-4}-a^{-2}+a^{2})x$
$\mathbf{5_6}: (-a^{-24}-a^{-22}+a^{-20}+2a^{-18}-2a^{-14}+a^{-10}+a^{-8})x$
$\mathbf{5_7}: (-1+a^{-14}-2a^{-10}-a^{-8}+2a^{-6}+2a^{-4}-a^{-2}+a^{4})x$
$\mathbf{5_8}: a^{-22}-a^{-18}+2a^{-10}+(a^{-26}-2a^{-22}+2a^{-18}-a^{-14}-a^{-10})x^2$
$\mathbf{5_9}: a^{-14}+2a^{-2}-a^{6}+(-a^{-10}+2a^{-6}-3a^{-2}+a^{2})x^2$
$\mathbf{5_{10}}: (2+a^{-10}+a^{-8}-a^{-6}-2a^{-4}-a^{4}+a^{8})x$
$\mathbf{5_{11}}: -a^{-22}+a^{-18}-a^{-14}-a^{-10}+3a^{-6}+a^{-2}+(2a^{-10}-3a^{-6})x^2$
$\mathbf{5_{12}}: (a^{-20}-2a^{-16}-a^{-14}+2a^{-12}+a^{-10}-a^{-8}-a^{-6}+a^{-4}+a^{-2})x$
$\mathbf{5_{13}}: (2-a^{-12}+2a^{-8}+a^{-6}-2a^{-4}-2a^{-2}+2a^{2}-a^{6})x$
$\mathbf{5_{14}}: (-2a^{-18}-a^{-16}+2a^{-14}+3a^{-12}-2a^{-8}+a^{-4})x$
$\mathbf{5_{15}}: a^{-14}-a^{-10}-2a^{-6}+a^{-2}-a^{6}+(-a^{-10}+3a^{-6}-3a^{-2}+a^{2})x^2$
$\mathbf{5_{16}}: -2a^{-22}+a^{-18}+a^{-14}-2a^{-10}+(a^{-22}-2a^{-14}+2a^{-10}-a^{-6})x^2$
$\mathbf{5_{17}}: a^{-26}-2a^{-18}+a^{-14}+2a^{-10}+(-a^{-22}+3a^{-18}-2a^{-14}-a^{-10})x^2$
$\mathbf{5_{18}}: a^{-14}-a^{-10}+a^{-6}+3a^{-2}-a^{2}-a^{6}+(a^{-6}-4a^{-2}+2a^{2})x^2$
$\mathbf{5_{19}}: (a^{-20}-a^{-18}+a^{-14}+a^{-12}-2a^{-8}+a^{-4})x+(-a^{-16}+a^{-12})x^3$
$\mathbf{5_{20}}: (a^{-16}+a^{-12}-a^{-10}-a^{-8}+a^{-6})x+(-a^{-12}+a^{-8})x^3$
$\mathbf{5_{21}}: (3+a^{-10}+a^{-8}-a^{-6}-a^{-4}-2a^{4})x+(-1+a^{4})x^3$
$\mathbf{5_{22}}: (2-a^{-12}-a^{-2}+a^{2})x+(a^{-8}-a^{-4})x^3$
$\mathbf{5_{23}}: (-a^{-24}+2a^{-20}+a^{-18}-2a^{-16}-3a^{-14}+a^{-12}+2a^{-10}+a^{-8})x$
$\mathbf{5_{24}}: (-1-a^{-12}-a^{-10}+a^{-8}+3a^{-6}+a^{-4}-2a^{-2}+a^{4})x$
$\mathbf{5_{25}}: -a^{-22}+a^{-18}+2a^{-6}+(a^{-22}-a^{-18}-a^{-6})x^2$
$\mathbf{5_{26}}: -a^{-18}+a^{-10}+a^{-2}+a^{2}+(a^{-14}-2a^{-10}+2a^{-6}-2a^{-2})x^2$
$\mathbf{5_{27}}: a^{-26}-a^{-22}-3a^{-18}+a^{-14}+a^{-10}-a^{-6}+(-a^{-22}+4a^{-18}-3a^{-14})x^2$
$\mathbf{5_{28}}: a^{-18}-3a^{-14}-2a^{-10}+2a^{-6}+(-a^{-18}+2a^{-14}+a^{-10}-2a^{-6})x^2$

Table 1. Cont'd. Kauffman polynomials of knots shown in Fig. 15

$\mathbf{5_{29}}: -2a^{-10}+a^{-6}+2a^{-2}-2a^{2}-a^{6}+(a^{-10}-3a^{-2}+2a^{2})x^{2}$
$\mathbf{5_{30}}: (-1+a^{-14}-2a^{-10}+2a^{-6}+a^{-4}-2a^{-2}+a^{2}+a^{4})x$
$\mathbf{5_{31}}: (1-a^{-12}-a^{-10}+2a^{-8}+2a^{-6}-a^{-4}-2a^{-2}+2a^{2}-a^{6})x$
$\mathbf{5_{32}}: -a^{-18}-a^{-14}+2a^{-10}+a^{-6}+a^{2}+(2a^{-14}-3a^{-10}+a^{-6}-a^{-2})x^{2}$
$\mathbf{5_{33}}: -2a^{-22}+a^{-18}+2a^{-14}+a^{-6}+(a^{-22}-2a^{-14}+a^{-10}-a^{-6})x^{2}$
$\mathbf{5_{34}}: (a^{-8}+a^{-6}-a^{-4}-2a^{-2}+a^{2}+a^{4})x$
$\mathbf{5_{35}}: (-1-a^{-10}+a^{-8}+2a^{-6}-2a^{-2}+a^{2}+a^{4})x$
$\mathbf{5_{36}}: (-a^{-18}+2a^{-14}+a^{-12}-2a^{-10}-2a^{-8}+a^{-6}+2a^{-4})x$
$\mathbf{5_{37}}: (2+a^{-8}-2a^{-4}-a^{-2}+2a^{2}-a^{6})x$
$\mathbf{5_{38}}: (a^{-16}+a^{-14}-a^{-12}-3a^{-10}-a^{-8}+2a^{-6}+2a^{-4})x$
$\mathbf{5_{39}}: (3+a^{-10}+a^{-8}-a^{-6}-3a^{-4}-a^{-2}+2a^{2}-a^{6})x$
$\mathbf{5_{40}}: (-1-a^{-16}-a^{-12}-a^{-10}+a^{-6})x+(a^{-12}-a^{-8}+a^{-4})x^{3}$
$\mathbf{5_{41}}: (-a^{-12}-a^{-4}-a^{-2}+a^{2}-a^{4})x+(1+a^{-8}-a^{-4})x^{3}$
$\mathbf{5_{42}}: (2+a^{-10}-a^{-6}-3a^{-4}-2a^{4})x+(-1+a^{-4}+a^{4})x^{3}$
$\mathbf{5_{43}}: (3+a^{-8}-a^{-6}-2a^{-4}+2a^{2}-a^{4}-a^{6})x$
$\mathbf{5_{44}}: (a^{-16}-a^{-12}-2a^{-10}+2a^{-6}+a^{-4})x$
$\mathbf{5_{45}}: (2+a^{-10}+a^{-8}-a^{-6}-2a^{-4}-a^{-2}+a^{2})x$
$\mathbf{5_{46}}: (a^{-14}+a^{-12}-2a^{-10}-2a^{-8}+2a^{-4}+a^{-2})x$
$\mathbf{5_{47}}: -a^{-10}+2a^{-6}+2a^{-2}-a^{2}+(a^{-10}-a^{-6}-2a^{-2}+a^{2})x^{2}$
$\mathbf{5_{48}}: a^{-14}-a^{-10}-a^{-6}+3a^{-2}+a^{2}-a^{6}+(-a^{-10}+3a^{-6}-4a^{-2}+a^{2})x^{2}$
$\mathbf{5_{49}}: a^{-18}-2a^{-14}+3a^{-6}+(-a^{-18}+2a^{-14}-2a^{-6})x^{2}$
$\mathbf{5_{50}}: -a^{-18}-2a^{-14}+2a^{-10}+3a^{-6}+(2a^{-14}-2a^{-10}-a^{-6})x^{2}$
$\mathbf{5_{51}}: (-a^{-18}+2a^{-14}+a^{-12}-a^{-8}+a^{-4}-a^{-2})x+(-a^{-10}+a^{-6})x^{3}$
$\mathbf{5_{52}}: (1+a^{-8}+a^{-6}-a^{-4}-a^{6})x+(-a^{-2}+a^{2})x^{3}$
$\mathbf{5_{53}}: (-1-3a^{-10}+3a^{-6}+a^{-4}-a^{-2}+a^{2}+a^{4})x+(a^{-10}-a^{-6})x^{3}$
$\mathbf{5_{54}}: a^{-18}+a^{-6}+(-a^{-18}-a^{-14}+a^{-10})x^{2}+(a^{-14}-a^{-10})x^{4}$
$\mathbf{5_{55}}: a^{-22}-a^{-18}+2a^{-10}+(-3a^{-22}+3a^{-18}-a^{-10})x^{2}+(a^{-22}-a^{-18})x^{4}$
$\mathbf{5_{56}}: a^{-14}+2a^{-2}-a^{6}+(-2a^{-10}+a^{-6}-2a^{-2}+2a^{2})x^{2}+(a^{-6}-a^{-2})x^{4}$
$\mathbf{5_{57}}: a^{-6}+a^{-2}+(-a^{-10}-a^{-6}+a^{2})x^{2}+(a^{-6}-a^{-2})x^{4}$
$\mathbf{5_{58}}: -a^{-10}+2a^{-2}+a^{2}+(a^{-10}+2a^{-6}-3a^{-2}-a^{2})x^{2}+(-a^{-6}+a^{-2})x^{4}$
$\mathbf{5_{59}}: -a^{-14}+a^{-10}+2a^{-6}-x^{2}a^{-18}+(a^{-14}-a^{-10})x^{4}$
$\mathbf{5_{60}}: -a^{-14}-a^{-2}+(a^{-14}+2a^{-6}+a^{-2})x^{2}-x^{4}a^{-6}$
$\mathbf{5_{61}}: -2a^{-22}+a^{-18}+a^{-14}-2a^{-10}+(a^{-22}-a^{-14}+4a^{-10})x^{2}-x^{4}a^{-10}$
$\mathbf{5_{62}}: a^{-14}-a^{-10}-2a^{-6}+a^{-2}-a^{6}+(-a^{-10}+4a^{-6}-a^{-2}+2a^{2})x^{2}-x^{4}a^{-2}$
$\mathbf{5_{63}}: -a^{-18}-2a^{-14}+a^{-10}+a^{-6}-a^{-2}+(2a^{-14}-a^{-10}+2a^{-6}+a^{-2})x^{2}-x^{4}a^{-6}$
$\mathbf{5_{64}}: a^{-6}-2a^{-2}-2a^{2}+a^{6}+(3a^{-2}+2a^{2}-a^{6})x^{2}-x^{4}a^{-2}$
$\mathbf{5_{65}}: -a^{-10}-a^{-6}+(2a^{-6}+a^{-2}+a^{2})x^{2}-x^{4}a^{-2}$
$\mathbf{5_{66}}: -2a^{-10}+a^{-6}+3a^{-2}+(a^{-10}-3a^{-2}+a^{2})x^{2}$
$\mathbf{5_{67}}: a^{-14}-2a^{-10}+4a^{-2}-a^{6}+(2a^{-6}-5a^{-2}+2a^{2})x^{2}$
$\mathbf{5_{68}}: -a^{-22}-a^{-18}+2a^{-14}+2a^{-10}+(2a^{-18}-2a^{-14}-a^{-10})x^{2}$
$\mathbf{5_{69}}: (-a^{-12}+3a^{-8}+2a^{-6}-2a^{-4}-4a^{-2}+2a^{2}+a^{4})x$

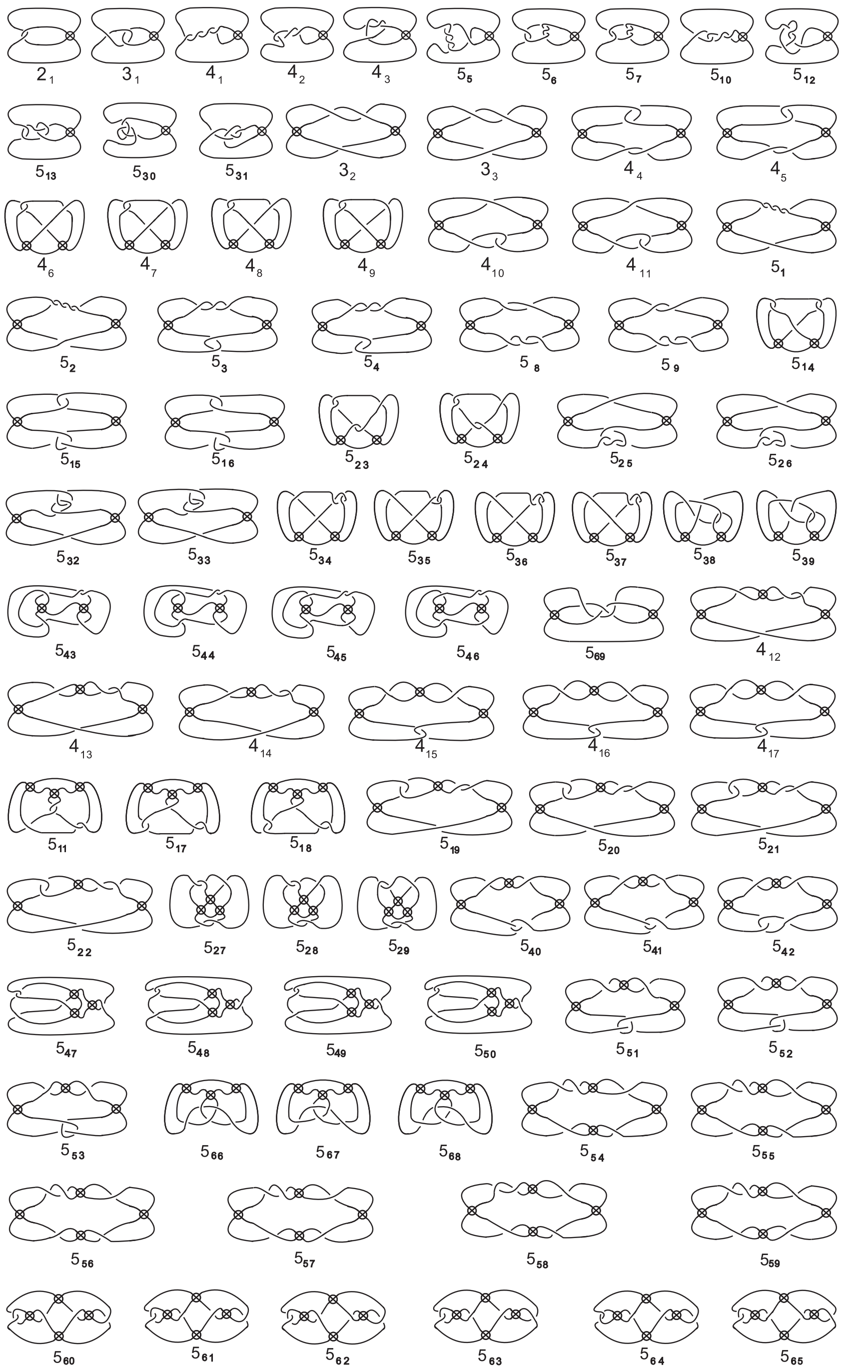

Fig. 16. Genus 1 prime virtual knots with at most 5 classical crossings